



**HAL**  
open science

# Mapping Earthquakes in Malawi Using Incorporated Research Institutions for Seismology (IRIS) Catalogue for 1972-2021

Polina Lemenkova

► **To cite this version:**

Polina Lemenkova. Mapping Earthquakes in Malawi Using Incorporated Research Institutions for Seismology (IRIS) Catalogue for 1972-2021. Malawi Journal of Science and Technology, 2021, 13 (2), pp.32-51. 10.5281/zenodo.5771582 . hal-03474728

**HAL Id: hal-03474728**

**<https://hal.science/hal-03474728>**

Submitted on 10 Dec 2021

**HAL** is a multi-disciplinary open access archive for the deposit and dissemination of scientific research documents, whether they are published or not. The documents may come from teaching and research institutions in France or abroad, or from public or private research centers.

L'archive ouverte pluridisciplinaire **HAL**, est destinée au dépôt et à la diffusion de documents scientifiques de niveau recherche, publiés ou non, émanant des établissements d'enseignement et de recherche français ou étrangers, des laboratoires publics ou privés.



Distributed under a Creative Commons Attribution - NonCommercial 4.0 International License

# Mapping Earthquakes in Malawi Using Incorporated Research Institutions for Seismology (IRIS) Catalogue for 1972-2021

Polina Lemenkova <sup>1,2\*</sup>

<sup>1</sup> Université Libre de Bruxelles, École polytechnique de Bruxelles (Brussels Faculty of Engineering), Laboratory of Image Synthesis and Analysis (LISA). Building L, Campus de Solbosch, Avenue Franklin Roosevelt 50, Brussels 1000, Belgium.

<sup>2</sup> Schmidt Institute of Physics of the Earth, Russian Academy of Sciences (RAS), Department of Natural Disasters, Anthropogenic Hazards and Seismicity of the Earth, Laboratory of Regional Geophysics and Natural Disasters (Nr. 303), Bolshaya Gruzinskaya St, 10, Bld. 1, Moscow, 123995, Russia.

\* **Corresponding Author Emails:** [polina.lemenkova@ulb.be](mailto:polina.lemenkova@ulb.be) and [pauline.lemenkova@gmail.com](mailto:pauline.lemenkova@gmail.com)

## Abstract

Cartographic data visualization is crucial for geological mapping in seismically active areas of Malawi. Representation of the datasets from IRIS database is beneficial for hazard risk assessment, forecasting and damage mitigation, especially for mapping the distribution and magnitude of earthquakes. Scripting cartography using Generic Mapping Tools (GMT) was used to map seismicity in Malawi Rift Zone based on IRIS catalogue for 1972–2021. The maps show relations among the elevation heights, distribution of seismic events and volcanos in the north of the Malawi Lake. The results show correlation between elevations and seismicity with local topographic depressions. Seismic data show variability of the seismicity level with more earthquakes recorded in the north of the country. This paper contributes to the regional studies of Malawi for risk assessment and geological hazard analysis.

**Keywords:** *Malawi, earthquakes, GMT, seismicity, Malawi Rift Zone*

Received: February 19, 2021, Accepted: August 30, 2021

## 1. Introduction

Mapping geologic and topographic data using advanced approaches is an important tool in Earth science. Effective visualization allows to identify geophysical processes in seismically active and geologically complex regions, such as Malawi (Ring *et al.*, 1992; Macheyeke *et al.*, 2015; Dawson *et al.*, 2018; Chisenga *et al.*, 2019; Bergé-Nguyen *et al.*, 2021). Besides, up-to-date maps enable to assess deformation consequences of seismic events, analyze

frequency, magnitude and focal depths of earthquakes in Malawi (Camelbeek & Iranga, 1996; Biggs *et al.*, 2010; Hamiel *et al.*, 2012; Accardo *et al.*, 2017). Finally, mapping enables to bring raw spatial data for environmental modeling and management of the country.

Visualizing, studying and analysis earthquakes has applications not only to the pure geophysical research yet also in practical cases of hazard risk monitoring, seismic risk assessment, modeling and prognosis with aim of mitigation of social consequences of earthquakes (Ngoma *et al.*, 2019). In perspective, scripting in cartography will play a key role due to the following reasons: i) GMT is an open source toolset which is a significant advantage; ii) Quicker data processing by scripting results in automatization; iii) Generation of new data, updated maps and dissemination of knowledge on seismicity.

Promising potential of scripting based cartographic data visualization in support of geological and hazard risk mapping (seismicity) is not yet sufficiently explored in the existing literature compared to the actuality of this topic. Specifically for Malawi, the applications of GMT is absent. In view of the above said, this research presents a significant contribution in both technical development of cartographic methodology and integrated visualization of the seismicity and topography using high-resolution data sources (events recorded for 1972-2021 from the IRIS data base and covering Malawi, topographic GEBCO grid).

The aim of this paper is mapping seismic setting of Malawi using scripting cartography of GMT because of advantages of automatization. Advanced mapping contribute to better understanding of the seismicity in Malawi. Compared with GIS based studies (Schenke & Lemenkova, 2008; Klaučo *et al.*, 2013), scripting methods of Generic Mapping Tools (GMT) present is a new technique. Compared to other techniques, the GMT brings significant advantages to mapping due to the automatization of geodata processing by scripts using machine learning approach (Lemenkova, 2019a). Besides that, the paper also describes the general mechanisms and processes of rifting in the Great Rift Valley regarding Malawi.

Reliable high-resolution topographic DEM and seismic data enables to perform spatial analysis that shows intricate pattern of topographic and seismic data reflecting very diversified deep structure of the Malawi Rift Zone region as a part of the Great Rift Valley. Besides, data integration enables to assess the complexity of geophysical setting in the Malawi Rift, and its relation with topography, seismicity and geology (Hopper *et al.*, 2020).

Location, magnitude, repeatability and distribution of earthquakes in Malawi are susceptible to both geological and tectonic drivers and occur over a range of spatial and temporal scales. Hence, complex geological analysis requires high-resolution data. The data used for GMT-based mapping include General Bathymetric Chart of the Oceans (GEBCO) which

presents the most comprehensive topographic data of the Earth used in geosciences (Gauger *et al.*, 2007; Lemenkova, 2020b; Fujii *et al.*, 2020).

## **2. Study Area, Data and Methods**

Malawi has complex geological setting formed as a result of long tectonic evolution of the East Africa largely influenced by the Great Rift Valley and formed Malawi rift and the Rungwe Volcanic Province (O'Donnell *et al.*, 2016; Borrego *et al.*, 2018; Accardo *et al.*, 2018). The Great Rift Valley crosses the country from N to S and includes the Malawi (Nyasa) Lake (Scholz *et al.*, 2011). The location of Malawi on the outskirts of the Precambrian African platform determines the mountainous character of its relief and crustal thickness structure (Tugume *et al.*, 2012; Wang *et al.*, 2019). The geological and geomorphological setting with rocks exposed at surface, divided into horsts and grabens control the availability of mineral resources which include deposits of coal, iron ores, and bauxites (Dill *et al.*, 2005; Dill, 2007).

Tectonically, the Malawi Rift is located at the southernmost segment of the Western Branch of the East African Rift System. The rift comprises several separate sub-basins showing an asymmetric half-graben (Ebinger *et al.*, 1987). There are seven found linked half-graben units in the Malawi Rift with the thickest sedimentary segments and greatest topography of flanking uplifts in the northern half-graben units (Specht & Rosendahl, 1989).

The Malawi Rift is an active, magma-poor, weakly extended continental rift stretching over 800 km from the Rungwe Volcanic Province in the north to the Urema Graben (Mozambique) in the south. The Lake Malawi is structurally divided by a sets of grabens into the three basins (North, Central and South), as a result of the tectonic movements. These parts are connected via transfer zones (Scholz *et al.*, 1989) but have distinct structure.

Central Basin is presented by the fault-bounded depression. Its West and East parts are expressed by the valley of the Luangwa River (Fig. 1) and Ruhuhu Basin. These depression show the Karoo rift basin as a sequence of sedimentary units, mostly of non-marine origin with occasional inclusions of marine to continental facies (Johnson *et al.*, 1996). The slowest seismic velocities occur within the Central Basin where sedimentary strata overlie Karoo group sediments (Catuneanu & Elango, 2001).

Southern part of the Malawi Rift has the main faults and connected zones of deeply fractured bedrock extending SW from the Bantyre. The region of Bantyre has two main gneiss types as remnants of the Basement Complex formed since Pre-Cambrian: pyroxene granulite gneiss and syenitic gneiss. Southern and central regions of the Lake Malawi are characterized by thick, acoustically transparent sediment and are most widespread in the offshore basins of these regions (Johnson & Davis, 1989).

Northern end of the Malawi Rift includes the Rungwe Volcanic Province, one of the four volcanic centers within the Western Branch of the East African Rift System (Furman, 2007). It is a place of the southernmost volcanism in the entire East African Rift System. The geomorphology of this region reflects the processes of active tectonism and earlier geologic evolution of the Malawi Rift Zone (Zhao *et al.*, 1997).

## 2.2 Data and Methods

### Data

In this study, the seismicity in Malawi and topographic pattern were examined from the GEBCO DEM and IRIS dataset archives and GMT scripting (Tables 1 and 2). The study employed two major data sources. The first database is formed by the General Bathymetric Chart of the Oceans (GEBCO) grid (Schenke, 2016) which presents the global terrain models for ocean and land (<https://www.gebco.net/>). The GEBCO grid was used to map the topography of Malawi. During the data inspection, the data census of GEBCO DEM was clipped for the study area and assessed using GDAL as follows: ‘gmt grdcut GEBCO\_2019.nc -R32/36/-17.5/-9 -Gmw\_relief.nc’ which resulted in trimmed area for Malawi and ‘gdalinfo -stats mw\_relief.nc’ which shown the statistical data range for the topography of Malawi: Minimum = 29 m, Maximum=2846 m, Mean=843 m, Standard Deviation (StdDev)=428 m.

The GEBCO grid is being constantly developing as an international project. By 2030, GEBCO Seabed 2030 is a collaborative project between GEBCO and the Nippon Foundation with the aim of constant improvement of the precision in the topographic coverage of the Earth. Therefore, the GEBCO grid in NetCDF format presents the most reliable and the up-to-date data for topographic mapping that was used in this study. Bitelli *et al.* (2018) argue that the accuracy and precision of the topographic data are crucial for mapping mountainous relief, such as impassable areas or complex geomorphological patterns. Lemenkova (2021a) also argues in a similar way regarding the topographic and bathymetric mapping.

The Incorporated Research Institutions for Seismology (IRIS) seismic data have been used in the analysis of major earthquakes in the monitored region of Malawi between 1972 and 2021 through the region of Malawi Lake where the tectonic activity cause higher seismicity due to the extent of the East African Rift System. The analysis is based on the determining the strongest earthquakes with higher magnitude (over 5.0), by processing the CSV table with IRIS data and converting data into the NGDC format compatible with GMT.

### 2.3 Methods

The combination of the high-resolution raster grids and reliable input data and advanced cartographic tools is the requirements for cartographic visualization. However, unlike in GIS-based studies, GMT-based scripting mapping differs in terms of technical approach, as demonstrated in Tables 1 and 2 where the scripts used for mapping are presented. Based on the applications of GMT, its approaches can be categorized into three classes: 1) cartographic visualization algorithms for traditional mapping (including design of mapping); 2) modelling algorithms (including processing data arrays and modelling graphical plots, e.g. geomorphological cross-sections); 3) statistical data analysis algorithms.

*Table 1: Script of the GMT used for Figure 1 (a): Topographic map of Malawi.*

No.	Commands of the GMT code	Meaning
1	<code>gmt grdimage mw_relief.nc -Cpauline.cpt -R32/36/-17.5/-9 -JM5.0i -I+a15+ne0.75 -t50 -Xc -P -K &gt; \$ps</code>	Make background transparent image
2	<code>gmt pscoast -R -J \ -Ia/thinner,blue -Na -N1/thick,dimgray -W0.1p -Df -O -K &gt;&gt; \$ps</code>	Add coastlines, borders, rivers
3	<code>gmt psclip -R32/36/-17.5/-9 -JM5.0i Malawi.txt -O -K &gt;&gt; \$ps</code>	clip the map by mask to only include country
4	<code>gmt grdimage mw_relief.nc -Cpauline.cpt -R32/36/-17.5/-9 -JM5.0i -I+a15+ne0.75 -Xc -P -O -K &gt;&gt; \$ps</code>	Add raster image
5	<code>gmt grdcontour mw_relief.nc -R -J -C500 -Wthinnest,darkbrown -O -K &gt;&gt; \$ps</code>	Add isolines
6	<code>gmt pscoast -R -J \ -Ia/thinner,blue -Na -N1/thick,dimgray -W0.1p -Df -O -K &gt;&gt; \$ps</code>	Add coastlines, borders, rivers
7	<code>gmt psclip -C -O -K &gt;&gt; \$ps</code>	Undo the clipping
8	<code>gmt psscale -Dg32/-17.9+w12.0c/0.15i+h+o0.3/0i+ml+e -R -J -Cpauline.cpt \ -Bg500f50a500+1"Colormap: 'turbo' Google's Improved Rainbow CPT [R=-3481/4326, H=0, C=HSV]" \ -I0.2 -By+lm -O -K &gt;&gt; \$ps</code>	Add color legend
9	<code>gmt psbasemap -R -J \</code>	Add grid

No.	Commands of the GMT code	Meaning
	<code>-Bpxg2f1a0.5 -Bpyg2f1a0.5 -Bsxg2 -Bsyg1 \</code> <code>-B+t"Topographic map of Malawi" -O -K &gt;&gt; \$ps</code>	
10	<code>gmt psbasemap -R -J \</code> <code>-Lx11.0c/-2.5c+c10+w75k+1"Mercator projection.</code> <code>Scale (km)" +f \</code> <code>-UBL/0p/-70p -O -K &gt;&gt; \$ps</code>	Add scalebar, directional rose
11	<code>gmt pstext -R -J -N -O -K \</code> <code>-F+jTL+f12p,26,blue2+jLB+a-306 &gt;&gt; \$ps &lt;&lt; EOF</code> <code>32.25 -12.1 Luangwa</code> <code>EOF</code>	Add texts
12	<code>gmt logo -Dx5.0/-3.1+o0.1i/0.1i+w2c -O -K &gt;&gt; \$ps</code>	Add GMT logo
13	<code>gmt pstext -R0/10/0/15 -JX10/10 -X0.5c -Y21.5c -N -</code> <code>O \</code> <code>-F+f10p,0,black+jLB &gt;&gt; \$ps &lt;&lt; EOF</code> <code>0.5 10.3 Digital elevation data: SRTM/GEBCO, 15 arc</code> <code>sec resolution grid</code> <code>EOF</code>	Add subtitle
14	<code>gmt psconvert Topo_MW.ps -A3.5c -E720 -Tj -Z</code>	Convert to image file using GhostScript

The first reason for using GMT toolset in this study is that it applies a certain syntax for its embedded language with pre-defined machine learning commands. This makes GMT similar to the programming languages (Lemenkov & Lemenkova, 2021) and contrasting from the traditional GIS. Using codes written for each of the cartographic elements plotted on the maps (see Tables 1 and 2) aims to automate the workflow. In this way, GMT uses the machine learning approach which has a high impact on the contemporary cartographic methods (Lemenkova, 2021b). This is caused by the technical advantages of the GMT-based mapping which results in the effective cartographic workflow: saving computer processing memory and time when handling with the multi-source datasets, automated procedures of mapping and increased speed of mapping where many operations are made by the machine rather than human-based operations. These technical advantages explain the choice of the GMT selected for this study.

The second reason of the choice of GMT the expansion of the big data in Earth science that requires special machine-based tools for speedy processing of the large volumes of spatial

data. Earthquakes in seismically active regions, such as the Earth African Rift, present in large numbers. Processing tables containing large numbers of such data (thousands of cells) require minimized handmade routine work and maximized machine learning approach, that can minimize errors for effective risk analysis. In contrast to the traditional GIS approaches, scripting based GMT can respond to such requirements. GMT present specific modules that have commands (so called ‘flags’ as demonstrated in Tables 1 and 2) forming cartographic algorithms that can be used to process data in two or more lines and plot a map in a rapid way.

In the GMT scripting, the ‘psxy’ module was used for mapping the variability of earthquakes, their magnitude and distribution over the country, that are entirely driven by the internal tectonic processes in the Great Rift Valley (Malawi segment).

*Table 2: Script of the GMT used for Figure 1 (b): Seismic map of Malawi*

<b>No</b>	<b>Commands of the GMT code</b>	<b>Meaning</b>
1	<code>gmt grdimage mw_relief.nc -Cpauline.cpt -R32/36/-17.5/-9 -JM5.0i -I+a15+ne0.75 -Xc -P -K &gt; \$ps</code>	Make raster image
2	<code>gmt psscale -Dg32/-17.85+w12.0c/0.15i+h+o0.3/0i+ml+e -R -J -Cpauline.cpt \ -Bg500f100a500+1"Color scale 'dem2' &lt;...&gt;" \ -I0.2 -By+lm -O -K &gt;&gt; \$ps</code>	Add legend
3	<code>gmt grdcontour mw_relief.nc -R -J -C1000 -Wthinner,gray12 -O -K &gt;&gt; \$ps</code>	Add isolines
4	<code>gmt pscoast -R -J -P \ -Ia/thinner,blue -Na -N1/thicker,khaki1 -W0.1p -Df -O -K &gt;&gt; \$ps</code>	Add coastlines, borders, rivers
5	<code>gmt psbasemap -R -J \ -Bpxg2fla1 -Bpyg2fla1 -Bsxg2 -Bsyg1 \ -B+t"Seismicity in Malawi: earthquakes 1972 to 2021" -O -K &gt;&gt; \$ps</code>	Add grid
6	<code>gmt psbasemap -R -J \ -Lx11.0c/-3.8c+c50+w100k+1"Mercator projection. Scale (km)" +f \ -UBL/0p/-110p -O -K &gt;&gt; \$ps</code>	Add scale, directional rose
7	<code>gmt psxy -R -J quakes_MW.ngdc -Wfaint -i4,3,6,6s0.1 -h3 -Scc -Csteps.cpt -O -K &gt;&gt; \$ps</code>	Add earthquake points



No	Commands of the GMT code	Meaning
8	gmt psxy -R -J volcanoes.gmt -St0.4c -Gred -Wthinnest -O -K >> \$ps	Add geological lines and points
9	gmt pslegend -R -J -Dx2.5/-3.2+w12.0c+o-2.0/0.1c \ -F+pthin+ithinner+gwhite -O -K << FIN >> \$ps H 10 Helvetica Seismicity: earthquakes magnitude (M) from 2.8 to 6.5. N 5 S 0.3c c 0.3c red 0.01c 0.5c M (6.3-6.5) <...> Volcanoes FIN	Add legend
10	gmt pstext -R0/10/0/15 -JX10/10 -X0.1c -Y21.5c -N -O - F+f1 1p,25,black+jLB >> \$ps << EOF -1.0 10.3 DEM: SRTM/GEBCO, 15 arc sec grid. Earthquakes: IRIS Seismic Event Database EOF	Add subtitle
11	gmt psconvert Geol_MW.ps -A3.5c -E720 -Tj -Z	Convert to image file by GhostScript

Potentially, mapping earthquakes is an important task in the field of geologic risk analysis, seismic prognosis, Earth hazards mapping and geophysical modelling. Due to the wide distribution of earthquakes worldwide and in the East African Rift in particular, the problem of the effective and precise seismic mapping in real time regime has recently become a challenging topic. Mapping geologic hazards can help finding solutions in preventing risks, mitigating hazards and saving lives and property (Lemenkova *et al.*, 2012).

### 3. Results

Seismic events of varying magnitudes correlate with ruptures along the buried faults of Malawi. Active earthquakes are also associated with northern region of the Malawi Lake, e.g. shallow earthquake sequence in Karonga region of northern Lake Malawi (12.2009). Active seismicity in northern Malawi (Fig. 1) is explained by the tectonic, geophysical and geological setting. To ascertain the analysis of the earthquake events, a dataset of 1,000 events were collected from the IRIS seismological monitoring center covering Malawi region and surroundings (Fig. 1, 32°-36°E; 9°S-17,5°S). The earthquakes were identified as shallow events from 1972 to 2021, with magnitudes 2.8 to 6.5 that occur in general along the Malawi Rift Zone and several volcanoes in the norther of the country, Fig. 1 (b).

The earthquake events with the magnitudes over 5.5 show surfaces with the highest tectonic activity situated in the rift zone (Fig. 1), which is indicative of the length of the fault on which they occur. All the analyzed earthquakes in Malawi are shallow (below 70 km depth). In general, shallow-focused earthquakes, according to the U.S. Geological Survey, cause more damage compared to the deeper earthquakes. However, typical earthquakes in this region have moderate Richter Scale magnitude (below 6.0  $M_L$ ), which is consistent with the amplitude of waves recorded by seismographs observed by IRIS database (Table 3).

*Table 3: Earthquakes in Malawi base don IRIS database: fragment of table showing the largest earthquakes (magnitude>5.0), used for mapping Figure 1 (b): Seismic map of Malawi.*

Year	Month	Day	Time	Latitude	Longitude	Depth, km	Magnitude, Richter Scale ( $M_L$ )	Region	Timestamp
1985	5	14	18:11:08	-10.562	41.424	10	6.4	Comoros region	484942268
1989	3	10	21:49:45	-13.702	34.42	30.3	6.2	Malawi	605569785
2009	12	19	23:19:15	-10.108	33.818	6	6	Malawi	1261264755
1985	5	14	13:24:57	-10.61	41.423	10	6	Comoros region	484925097
2009	12	8	03:08:57	-9.948	33.878	8	5.9	Malawi	1260241737
2009	12	6	17:36:36	-10.126	33.87	9	5.8	Malawi	1260120996
2008	8	27	06:46:19	-10.751	41.469	10	5.7	Comoros region	1219819579
1989	3	9	02:37:00	-13.71	34.381	29.6	5.7	Malawi	605414220
1976	9	19	14:59:43	-11.056	32.857	27	5.7	Zambia	211993183
1985	6	28	07:32:20	-10.614	41.238	10	5.6	Comoros region	488791940
2009	12	12	02:27:03	-9.942	33.911	10	5.5	Malawi	1260584823
1989	9	5	20:49:34	-11.732	34.45	10	5.4	Malawi	621031774
1985	5	14	19:54:42	-10.705	41.345	10	5.4	Comoros region	484948482
1983	9	3	10:21:24	-15.386	41.385	10	5.4	Mozambique Channel	431432484
2014	11	2	18:25:40	10.9587	29.7368	10	5.3	49km NNE of Samfya, Zambia	1414952740
2010	8	3	19:42:13	-9.5	39.064	10	5.3	Tanzania	1280864533
2009	12	6	17:58:15	-10.171	33.968	10	5.3	Malawi	1260122295
1995	8	10	00:41:04	-15.473	41.604	10	5.3	Mozambique Channel	808015264

Year	Month	Day	Time	Latitude	Longitude	Depth, km	Magnitude, Richter Scale (M <sub>L</sub> )	Region	Timestamp
1985	5	30	08:32:17	-10.657	41.355	10	5.3	Comoros region	486289937
1975	2	15	06:16:27	-16.238	41.556	33	5.3	Mozambique Channel	161676987
2016	4	12	15:16:46	10.7675	41.4346	10	5.2	127km ESE of Madimba, Tanzania	1460474206
2015	7	15	14:10:04	15.6101	41.0503	14.6	5.2	72km SSE of Ilha de Mocambique, Mozambique	1436969404
2009	12	6	18:00:01	-10.024	33.866	10	5.2	Malawi	1260122401
2008	1	21	02:49:11	-10.534	41.556	10	5.2	Comoros region	1200883751
2002	8	31	22:52:33	-9.737	34.313	10	5.2	Lake Malawi region, Malawi-Tanzania	1030834353
2002	7	16	14:50:14	-11.65	41.071	10	5.2	Comoros region	1026831014
1982	4	29	20:20:20	-10.644	41.381	10	5.2	Comoros region	388959620
2018	6	5	22:55:28	-11.94	40.9658	10	5.1	59km NE of Ibo, Mozambique	1528239328
2014	12	31	19:47:36	10.0274	33.8632	14.9	5.1	12km SW of Karonga, Malawi	1420055256
2011	9	18	06:26:59	-16.17	42.158	10	5.1	Mozambique Channel	1316327219
2009	12	6	19:36:41	-10.105	33.947	10	5.1	Malawi	1260128201
2009	12	6	18:29:14	-10.131	33.915	10	5.1	Malawi	1260124154
2008	1	21	15:28:35	-10.566	41.571	10	5.1	Comoros region	1200929315
1995	7	22	13:31:53	-13.966	34.82	10	5.1	Malawi	806419913
1995	7	20	05:08:25	-12.402	41.41	10	5.1	Comoros region	806216905

*Impacts of improved traffic control measures on air quality and noise level in ...*

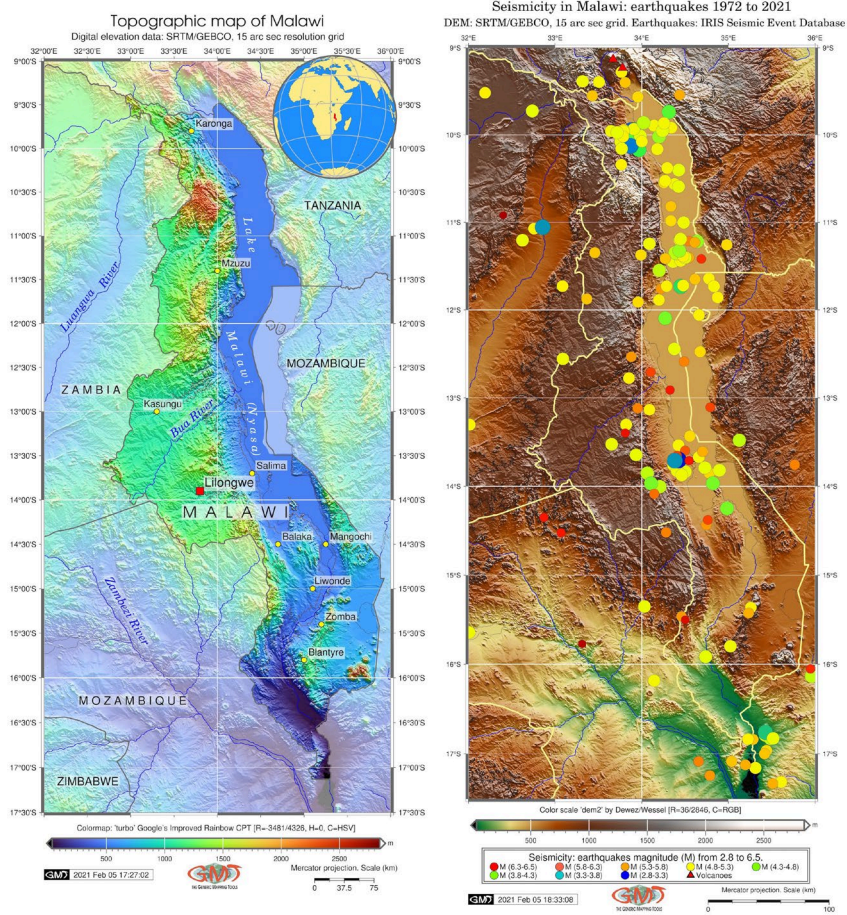
Year	Month	Day	Time	Latitude	Longitude	Depth, km	Magnitude, Richter Scale (M <sub>L</sub> )	Region	Timestamp
1990	2	28	20:05:31	-13.969	34.107	33	5.1	Malawi	636235531
1985	6	24	14:19:22	-10.713	41.159	10	5.1	Comoros region	488470762
1984	1	22	02:30:30	-14.249	34.984	10	5.1	Malawi	443586630
1978	1	8	06:31:52	-12.094	34.27	33	5.1	Malawi	253089112
1976	10	5	06:25:27	-10.946	41.295	33	5.1	Comoros region	213344727
2020	8	24	07:03:49	11.2191	34.6397	10	5	15 km S of Liuli, Tanzania	1598252629
2018	8	21	05:47:57	10.7251	41.3524	10	5	117km ESE of Madimba, Tanzania	1534830477
2017	3	29	20:37:03	10.9531	41.051	10	5	86km ENE of Mocimboa, Mozambique	1490819823
2012	2	13	00:49:31	-13.928	40.891	10	5	Mozambique	1329094171
2009	12	7	18:16:32	-9.998	33.844	10	5	Malawi	1260209792
2009	12	7	09:31:44	-10.113	33.837	10	5	Malawi	1260178304
2009	12	7	03:35:40	-10.132	33.908	10	5	Malawi	1260156940
2007	9	16	14:01:47	-11.812	42.082	3.1	5	Comoros region	1189951307
2007	6	18	23:51:10	-12.466	41.832	10	5	Comoros region	1182210670
2005	1	4	19:58:06	-10.407	41.494	29.4	5	Comoros region	1104868686
2005	1	4	19:44:12	-10.354	41.012	10	5	Comoros region	1104867852
2003	5	21	06:22:44	-10.021	34.199	29	5	Malawi	1053498164
1996	6	15	10:02:41	-16.461	41.638	10	5	Mozambique Channel	834832961
1989	1	1	17:16:41	-11.54	41.064	10	5	Comoros region	599678201
1985	9	17	10:57:10	-10.576	41.094	10	5	Comoros region	495802630
1985	6	24	14:04:44	-10.692	41.224	10	5	Comoros region	488469884
1985	6	24	13:41:24	-10.642	41.096	10	5	Comoros	488468484

Year	Month	Day	Time	Latitude	Longitude	Depth, km	Magnitude, Richter Scale ( $M_L$ )	Region	Timestamp
								region	
1980	2	18	07:00:44	-10.986	41.16	33	5	Comoros region	319705244
1979	11	4	21:12:00	-11.324	34.433	33	5	Malawi	310597920

After examination of the available IRIS data (the seismic events with maximal magnitude above 5.0  $M_L$  are shown in Table 3) it was concluded that the most earthquakes with maximal magnitude have a location in the center of the country along the Malawi Rift Zone, while the earthquakes with lower magnitude (pointed as yellow-colored points) are predominantly located in the north of the country. The red-colored points indicate higher magnitude of the earthquakes, and red triangle point at the volcanoes in the norther of Malawi.

The earthquake hazards are distributed differently over the years in period of 1972 to 2021: 4 events were recorded in 1973 with lower magnitude (4.3 to 4.9  $M_L$ ), only two events in 1974 (4.3  $M_L$  and 4.9  $M_L$ ), 11 earthquakes were detected in the period of 1976 to 1979. In contrast for the period of 1980 to 1990 75 shallow earthquakes (magnitudes 10 to 33) were recorded in the IRIS database with magnitudes 2.8  $M_L$  to 6.2  $M_L$  (here the earthquake with magnitude of 6.2  $M_L$  has been recorded on March 10, 1989).

The period of 1990 to 1999 is characterized by lesser seismic activity (only 35 events noted) with the majority of the events as shallow earthquakes (5 to 33 km). The deepest earthquakes are recorded (46.4 km) on August 24, 1998 with magnitude of 4.8  $M_L$  Richter Scale. The magnitude for the rest of the earthquakes during this period is from 3.4 to 5.1  $M_L$ . The period of 2000 to 2009 is analyzed based on the 60 events. The magnitude ranges from 3.7 to 6.0  $M_L$  Richter Scale with the strongest earthquake (6.0  $M_L$ ) in December 19, 2009. The recent period (2010 to 2021) presents 45 events with variations of magnitude from 3.9  $M_L$  Richter Scale (November 2, 2017 at depth 10 km) to 5.1 (12 km SW of Karonga, Malawi) at depth of 14.9 km on December 31, 2014.



(a)

(b)

Figure 1: Topographic map and seismicity of Malawi. Earthquakes data: IRIS. Earthquake depths range: 1.1. to 46.4 km. Magnitude: 2.8 to 6.5. Mapping: GMT. Source: author.

The data have been received based on the IRIS stations and determined from the data recorded by seismometers using the vibrations from earthquakes that travel through the Earth as recorded ground motions (shaking of the ground beneath the earthquakes). The dataset covers the period of 1972 to 2021, Figure 1 (b). The results of the visualization of earthquakes in Malawi based on the IRIS seismological monitoring database and GMT visualization are presented in Figure 1 (b).

#### 4. Discussion

Regular monitoring and mapping of the geological and geophysical settings using high-resolution data and advanced cartographic solutions are one of the prime challenges in

studying such seismically active region as Malawi. Accurate and automated mapping enables to investigate the relationships between deep geodynamic processes causing earthquakes and subsurface geological setting reflected in topography of the country. In recent decades rapid development of the machine learning and computing technologies significantly influenced the cartographic development and strategies of data visualization that were adopted in this study by the application of GMT advanced scripting toolset for mapping seismicity of Malawi.

The presented GMT based mapping adopted scripting strategy which is similar to the programming in its principal technical concept (Lemenkova, 2019b). Several GMT modules have been used for plotting maps and processing seismic data. These included ‘grdcut’, ‘gdalinfo’, ‘grdimage’, ‘psxy’, ‘psscale’, ‘pscoast’, ‘psbasemap’, ‘grdcontour’ and some minor GMT modules, as also demonstrated in details in Tables 1 and 2. In addition, cartographic workflow was better performed by significant automation of the data processing, smooth and flexible data formatting, compatibility of GMT with GDAL and high-resolution IRIS and GEBCO data.

The findings revealed a link between the topography and geologic setting affecting the distribution of the earthquakes over Malawi, with the majority of seismic events being located in the Malawi Rift Zone and in the northern region of the country. Between 1972 and 2021, the main earthquake hazards in Malawi were a combination of shallow and moderate events situated in the Malawi Rift Zone and caused by the geophysical setting and active tectonics. Diversified topographic pattern of Malawi that is notable for Malawi Rift Zone and the surrounding landscapes has been demonstrated using GEBCO grid. Seismicity in Malawi continue to present certain geologic risks, especially due to the shallow depth of the majority of the earthquake events.

## **5. Conclusion**

The study presented the machine learning cartographic approach of GMT aimed at investigating the relationship of the seismicity and topographic elevation based on analysis of the complex geodynamic and tectonic factors in Malawi Rift Zone. The performed GMT-based data interpretation enabled to highlight southern and northern sectors of Malawi generally characterized by different seismic setting according to the earthquake distribution and magnitude and focal depth.

The application of machine learning scripting techniques of GMT to mapping seismicity of Malawi has presented in this paper. This research reviews the tectonic setting in the Malawi Rift Zone as a part of the East African Rift System, and reports recent advances achieved in cartographic methods of mapping. Then it puts forward advantages and prospects of GMT based mapping compared to the traditional GIS by providing scripts and explaining the approach of coding and programming for future similar cartographic works in the field.

The primary contributions of this research can be summarized as follows:

1. Machine learning spatial data handling by GMT performs workflow automatically from which enables to overcome the difficulty of manual routine of mapping.
2. The presented cartographic methodology supported by the two scripts (Tables 1 and 2) can achieve the print-quality automated GMT-based mapping in similar works. The GMT-based mapping effectively achieves batch scripting which significantly increases the speed of mapping and minimizes human-induced errors in cartographic plotting.
3. Automatization of the cartographic mapping enables to meet the needs of geological and seismic mapping, because it enables to present mapping in fast and operative way and can contribute to risk analysis and seismic prognosis.
4. The GMT operates with various formats of data which enabled to import the IRIS seismic data for processing and visualization.
5. The GMT-based mapping greatly improves visual efficiency and design of maps. It has extensive embedded colour palettes which improves the presentation and readability of geologic hazards maps.
6. The presented maps indicate that the GMT-based method of mapping achieves fine cartographic performance in terms of both qualitative visual design and quantitative evaluation of seismic events which makes is suitable for geologic risk analysis.
7. The GMT-based scripting methods of mapping and cartographic data processing achieved through machine learning presents a promising and perspective trend in the geologic mapping of such seismically active regions as Malawi Rift Zone (see Table 3) and the East African Rift System.

Using GMT cartographic toolset this study analyzed the distribution, depth and magnitude of the series off earthquakes experienced and recorded for Malawi Rift Zone during the period of 1972 to 2021 to provide insights on the spatial topographic distribution and strength of earthquakes over Malawi. To this end, the study explored how different seismicity in Malawi was over the decades and presented an overview for the shorter 10-year periods of 1972 to 1979, and soon until 2010 to 2021. The seismic events have been recorded as shallow with depths below 70 km. The magnitude ranges from 2.8 to 6.5  $M_L$  Richter Scale.

In conclusion, automated mapping performed using GMT presents a strong potential for future applications in seismic and geological mapping of Malawi. The presented scripts can be re-used in similar research with regional adjustments and environmental focus.



## Acknowledgements

This research has been implemented into the framework of the project No. 0144-2019-0011, Schmidt Institute of Physics of the Earth, Russian Academy of Sciences. The author thanks the MJST Chief Editor Prof. Dr. Cosmo Ngongondo, and three anonymous reviewers for comments, remarks and corrections during the review of this manuscript.

## References

- Accardo, N.J., Gaherty, J.B., Shillington, D.J., Ebinger, C.J., Nyblade, A.A., Mbogoni, G.J., Chindandali, P.R.N., Ferdinand, R.W., Mulibo, G.D., Kamihanda, G., Keir, D., Scholz, C., Selway, K., O'Donnell, J.P., Tepp, G., Gallacher, R., Mtelela, K., Salima, J. & Mruma, A. (2017). Surface wave imaging of the weakly extended Malawi Rift from ambient-noise and teleseismic Rayleigh waves from onshore and lake-bottom seismometers. *Geophysical Journal International* **209(3)**: 1892–1905.
- Accardo, N.J., Shillington, D.J., Gaherty, J.B., Scholz, C.A., Nyblade, A.A., Chindandali, P. R.N., Kamihanda G., McCartney T., Wood D. & Wambura Ferdinand, R. (2018). Constraints on Rift Basin structure and border fault growth in the northern Malawi Rift from 3-D seismic refraction imaging. *Journal of Geophysical Research: Solid Earth* **123**: 10003–10025.
- Bergé-Nguyen, M., Cretaux, J.-F., Calmant, S., Fleury, S., Satylkanov, R., Chontoev, D. & Bonnefond, P. (2021). Mapping mean lake surface from satellite altimetry and GPS kinematic surveys. *Advances in Space Research* **67(3)**: 985–1001.
- Biggs, J., Nissen, E., Craig, T., Jackson, J. & Robinson, D. (2010). Breaking up the hanging wall of a rift-border fault: the 2009 Karonga earthquakes, Malawi. *Geophysical Research Letters* **37(11)**: L11305.
- Bitelli, G., Roncari, G., Tini, M.A. & Vittuari, L. (2018). High-precision topographical methodology for determining height differences when crossing impassable areas. *Measurement* **118**: 147-155.
- Borrego, D., Nyblade, A.A., Accardo, N.J., Gaherty, J.B., Ebinger, C.J., Shillington, D.J., Chindandali, P.R.N., Mbogoni, G., Wambura, R., Mulibo, F.G., O'Donnell, J.P., Kachingwe, M. & Tepp, G. (2018). Crustal structure surrounding the northern Malawi rift and beneath the Rungwe Volcanic Province, East Africa. *Geophysical Journal International* **215(2)**: 1410–1426.

- Camelbeeck, T. & Iranga, M.D. (1996). Deep crustal earthquakes and active faults along the Rukwa trough, eastern Africa. *Geophysical Journal International* **124**(2): 612–630.
- Chisenga, C., Dulanya, Z. & Jianguo, Y. (2019). The structural re-interpretation of the Lower Shire Basin in the Southern Malawi rift using gravity data. *Journal of African Earth Sciences* **149**: 280–290.
- Dawson, S.M., Laó-Dávila, D.A., Atekwana, E.A. & Abdelsalam, M.G. (2018). The influence of the Precambrian Mughese Shear Zone structures on strain accommodation in the northern Malawi Rift. *Tectonophysics* **722**: 53–68.
- Dill, H.G., Ludwig, R.-R., Kathewera, A. & Mwenelupembe, J. (2005). A lithofacies terrain model for the Blantyre Region: Implications for the interpretation of palaeosavanna depositional systems and for environmental geology and economic geology in southern Malawi. *Journal of African Earth Sciences* **41**(5): 341–393.
- Dill, H.G. (2007). A review of mineral resources in Malawi: With special reference to aluminium variation in mineral deposits. *Journal of African Earth Sciences* **47**(3): 153–173.
- Ebinger, C.J., Rosendahl, B.R. & Reynolds, D.J. (1987). Tectonic model of the Malaŵi rift, Africa. *Tectonophysics* **141**(1–3): 215–235.
- Fujii, Y., Satake, K., Watada, S. & Ho, T.-C. (2020). Slip distribution of the 2005 Nias earthquake (Mw 8.6) inferred from geodetic and far-field tsunami data. *Geophysical Journal International* **223**(2): 1162–1171.
- Gauger, S., Kuhn, G., Gohl, K., Feigl, T., Lemenkova, P. & Hillenbrand, C. (2007). Swath-bathymetric mapping. *Reports on Polar and Marine Research* **557**: 38–45.
- González-Castillo, L., Junge, A., Galindo-Zaldívar, J. & Löwer, A. (2015). Influence of a narrow strait connecting a large ocean and a small sea on magnetotelluric data: Gibraltar Strait. *Journal of Applied Geophysics* **122**: 103–110.
- Hamiel, Y., Baer, G., Kalindekafe, L., Dombola, K. & Chindandali, P. (2012). Seismic and aseismic slip evolution and deformation associated with the 2009–2010 northern Malawi earthquake swarm, East African Rift. *Geophysical Journal International* **191**(3): 898–908.
- Hopper, E., Gaherty, J.B., Shillington, D.J., Accardo, N.J., Nyblade, A.A., Holtzman, B.K., Havlin, C., Scholz, C.A., Chindandali, P.R.N., Ferdinand, R.W., Mulibo, G.D. & Mbogoni, G. (2020). Preferential localized thinning of lithospheric mantle in the melt-poor Malawi Rift. *Nature Geoscience* **13**: 584–589.

- Johnson, T.C. & Davis, T.W. (1989). High resolution seismic profiles from Lake Malawi, Africa. *Journal of African Earth Sciences (and the Middle East)* **8(2–4)**: 383–392.
- Johnson, M.R., Van Vuuren, C.J., Hegenberger, W.F., Key, R. & Shoko, U. (1996). Stratigraphy of the Karoo Supergroup in southern Africa: an overview. *Journal of African Earth Sciences* **23(1)**: 3–15.
- Klaučo, M., Gregorová, B., Stankov, U., Marković, V. & Lemenkova, P. (2013). Determination of ecological significance based on geostatistical assessment: a case study from the Slovak Natura 2000 protected area. *Open Geosciences* **5(1)**: 28–42.
- Lemenkov, V. & Lemenkova, P. (2021). Using TeX Markup Language for 3D and 2D Geological Plotting. *Foundations of Computing and Decision Sciences* **46(3)**: 43–69.
- Lemenkova, P. (2011). *Seagrass Mapping and Monitoring Along the Coasts of Crete, Greece*. M.Sc. Thesis. Netherlands: University of Twente. 158 pp.
- Lemenkova, P., Promper, C. & Glade, T. (2012). Economic Assessment of Landslide Risk for the Waidhofen a.d. Ybbs Region, Alpine Foreland, Lower Austria. In: Eberhardt, E., Froese, C., Turner, A. K. & Leroueil, S. (Eds.). *Protecting Society through Improved Understanding*.
- 11<sup>th</sup> International Symposium on Landslides & the 2<sup>nd</sup> North American Symposium on Landslides & Engineered Slopes (NASL), June 2–8, 2012. Canada, Banff, 279–285.
- Lemenkova, P. (2019a). GMT Based Comparative Analysis and Geomorphological Mapping of the Kermadec and Tonga Trenches, Southwest Pacific Ocean. *Geographia Technica* **14(2)**: 39–48.
- Lemenkova, P. (2019b). Statistical Analysis of the Mariana Trench Geomorphology Using R Programming Language. *Geodesy and Cartography* **45(2)**: 57–84.
- Lemenkova, P. (2020a). Applying Automatic Mapping Processing by GMT to Bathymetric and Geophysical Data: Cascadia Subduction Zone, Pacific Ocean. *Journal of Environmental Geography* **13(3-4)**: 15–26.
- Lemenkova, P. (2020b). GEBCO Gridded Bathymetric Datasets for Mapping Japan Trench Geomorphology by Means of GMT Scripting Toolset. *Geodesy and Cartography* **46(3)**: 98–112.

- Lemenkova, P. (2021a). Topography of the Aleutian Trench south-east off Bowers Ridge, Bering Sea, in the context of the geological development of North Pacific Ocean. *Baltica* **34(1)**: 27–46.
- Lemenkova, P. (2021b). Exploring structured scripting cartographic technique of GMT for ocean seafloor modeling: A case of the East Indian Ocean. *Maritime Technology and Research* **3(2)**: 162–184.
- Macheyeki, A.S., Mdala, H., Chapola, L.S., Manhiça, V.J., Chisambi, J., Feitio, P., Ayele, A., Barongo, J., Ferdinand, R.W., Ogubazghi, G., Goitom, B., Hlatywayo, J.D., Kianji, G.K., Marobhe, I., Mulowezi, A., Mutamina, D., Mwano, J.M., Shumba, B. & Tumwikirize, I.
- (2015). Active fault mapping in Karonga-Malawi after the December 19, 2009 Ms 6.2 seismic event. *Journal of African Earth Sciences* **102**: 233–246.
- Ngoma, I., Kafodya, I., Kloukinas, P., Novelli, V., Macdonald, J. & Goda, K. (2019). Building Classification and Seismic Vulnerability of Current Housing Construction in Malawi. *Malawi Journal of Science and Technology* **11(1)**: 57–72.
- O'Donnell, J.P., Selway, K., Nyblade, A.A., Brazier, R.A., El Tahir, N. & Durrheim, R.J. (2016). Thick lithosphere, deep crustal earthquakes and no melt: a triple challenge to understanding extension in the western branch of the East African Rift. *Geophysical Journal International* **204(2)**: 985–998.
- Ring, U., Betzler, C. & Delvaux, D. (1992). Normal vs. strike-slip faulting during rift development in East Africa: *The Malawi Rift*. *Geology* **20(11)**: 1015–1018.
- Schenke, H. (2016). General Bathymetric Chart of the Oceans (GEBCO). In: Harff J., Meschede M., Petersen S., Thiede J. (eds). *Encyclopedia of Marine Geosciences*. Encyclopedia of Earth Sciences Series. Springer, Dordrecht.
- Schenke, H.W. & Lemenkova, P. (2008). Zur Frage der Meeresboden-Kartographie: Die Nutzung von AutoTrace Digitizer für die Vektorisierung der Bathymetrischen Daten in der Petschora-See. *Hydrographische Nachrichten* **81**: 16–21.
- Scholz, C.A., Rosendahl, B.R., Versfelt, J., Kaczmarick, K.J. & Woods, L.D. (1989). *Seismic Atlas of Lake Malawi*. Project PROBE, geophysical atlas series, **2**: 116.
- Scholz, C.A., Cohen, A.S., Johnson, T.C., King, J., Talbot, M.R. & Brown, E.T. (2011). Scientific drilling in the Great Rift Valley: The 2005 Lake Malawi Scientific Drilling Project — An overview of the past 145,000 years of climate variability in

Southern Hemisphere East Africa. *Palaeogeography, Palaeoclimatology, Palaeoecology* **303(1–4)**: 3-19.

Specht, T.D. & Rosendahl, B.R. (1989). Architecture of the Lake Malawi Rift, East Africa. *Journal of African Earth Sciences (and the Middle East)* **8(2–4)**: 355–382.

Suetova, I.A., Ushakova, L.A. & Lemenkova, P. (2005). Geoinformation mapping of the Barents and Pechora Seas. *Geography and Natural Resources* **4**: 138–142.

Tugume, F., Nyblade, A. & Julià, J. (2012). Moho depths and Poisson's ratios of Precambrian crust in East Africa: Evidence for similarities in Archean and Proterozoic crustal structure. *Earth and Planetary Science Letters* **355–356**: 73-81.

Wang, T., Feng, J., Liu, K.H. & Gao, S.S. (2019). Crustal structure beneath the Malawi and Luangwa Rift Zones and adjacent areas from ambient noise tomography. *Gondwana Research* **67**: 187-198.

Zhao, M., Langston, C.A., Nyblade, A.A. & Owens, T.J. (1997). Lower-crustal rifting in the Rukwa Graben, East Africa. *Geophysical Journal International* **129(2)**: 412–420.